INSTITUTE OF PHYSICS PUBLISHING JOURNAL OF PHYSICS: CONDENSED MATTER

J. Phys.: Condens. Matter **15** (2003) 3333–3342 PII: S0953-8984(03)59029-4

Raman scattering study of $Nd_{1-x}Sr_xMnO_3$ ($x = 0.3, 0.5$)

K-Y Choi[1], P Lemmens[1,2], G Güntherodt[1], M Pattabiraman[3], G Rangarajan[3], V P Gnezdilov[4], G Balakrishnan[5], D McK Paul[5] and M R Lees[5]

[1] 2. Physikalisches Institut, RWTH Aachen, 52056 Aachen, Germany
[2] MPI for Solid State Research, 70569 Stuttgart, Germany
[3] Department of Physics, Indian Institute of Technology, Madras, Chennai 600036, India
[4] B I Verkin Institute for Low Temperature Physics NASU, 61164 Kharkov, Ukraine
[5] Department of Physics, University of Warwick, Coventry CV4 7AL, UK

E-mail: ky.choi@physik.rwth-aachen.de

Received 3 February 2003
Published 6 May 2003
Online at stacks.iop.org/JPhysCM/15/3333

Abstract

We report on polarized Raman scattering of single crystals of $Nd_{1-x}Sr_xMnO_3$ ($x = 0.3, 0.5$). Raman spectra of $Nd_{0.7}Sr_{0.3}MnO_3$ show a significant change through the metal–insulator transition. In the ferromagnetic metallic phase phonon modes grow in intensity and number while the electronic continuum becomes more pronounced. We suggest that these effects are due to the strong competition between the localization and the delocalization of carriers which is the origin of the largest colossal magnetoresistance effect ever reported for the manganites. Raman spectra of $Nd_{0.5}Sr_{0.5}MnO_3$, upon cooling through the charge-ordering temperature $T_{CO} = 148$ K, exhibit several new lines which undergo a substantial hardening. This hardening is interpreted as a freezing of the Jahn–Teller distortions with a gradual decrease of a fraction of the ferromagnetic phase in the CE-type charge/orbital ordered state.

1. Introduction

The manganese perovskites $R_{1-x}A_xMnO_3$ (R = rare earth, A = alkaline earth) have attracted considerable attention in the context of strongly correlated systems in which the electronic, spin and/or lattice degrees of freedom interact strongly. They exhibit a variety of interesting phenomena like 'colossal magnetoresistance' (CMR) and complex phase diagrams including paramagnetic insulating (PI), ferromagnetic metallic (FM) and charge-ordered antiferromagnetic (AF) phases as a function of doping and temperature [1, 2]. The main physics of the CMR effect lies in a transition from the PI to the FM phase. The coexistence of ferromagnetism and the metallic state was explained in the framework of the double exchange (DE) model [3]. However, to account for a drastic change in resistivity and a low critical

temperature the DE model must be combined with magnetic and/or lattice polarons due to the Jahn–Teller (JT) distortion of MnO_6 octahedra which promote carrier localization and dress charge carriers via clouds of phonons [4, 5]. In addition, orbital degrees of freedom at different doping levels should be considered in order to understand the metal–insulator transition (MIT) and the rich phase diagram. Even at optimal doping ($x \simeq 0.3$–0.5) a novel type of orbital ordering or an orbital liquid are suggested in the metallic phase without accompanying lattice distortions [6]. Recently, there is accumulating evidence that a charge/lattice/orbital inhomogeneity and a concomitant phase separation play important roles in the CMR effects since carrier-rich regions grow in a magnetic field against carrier-poor regions leading to a large negative magnetoresistance [7].

With decreasing temperature the doped manganites with $x \sim 0.3$ undergo a transition from the PI to the FM while showing CMR phenomena around the transition. The largest CMR effect among the manganites has been reported in $Nd_{0.7}Sr_{0.3}MnO_3$ [8, 9]. In the FM phase of $Nd_{0.7}Sr_{0.3}MnO_3$ recent x-ray synchrotron measurements have revealed the presence of AF CE-type charge-/orbitally-ordered (COO) nanoclusters [10]. Inhomogeneous magnetism has been further observed by ^{55}Mn NMR measurements exhibiting strong carrier localization well below $T_c \approx 240$ K. In the CE phase ferromagnetic charge- and orbital-ordered zigzag chains are coupled antiferromagnetically to each other in the ab planes. The half-doped $Nd_{0.5}Sr_{0.5}MnO_3$ has a ground state as the CE phase. However, the energy difference between the CE, FM and AF phases is small [11]. As a result, strong fluctuations and phase segregation are expected. Actually, recent x-ray results reveal the coexistence of such phases in $Nd_{0.5}Sr_{0.5}MnO_3$ over a large temperature range extending to the PI and FM phases [12, 13].

Raman spectroscopy is sensitive to local electronic, lattice and spin degrees of freedom as well as coupling between them. Thus, it can provide valuable information about the phase separation via electron–phonon and spin–phonon interactions. In this paper, we report an inelastic light scattering study of $Nd_{1-x}Sr_xMnO_3$ ($x = 0.3, 0.5$). In spite of an intensive study of the manganites using Raman spectroscopy, these systems have not yet been fully addressed although $Nd_{0.7}Sr_{0.3}MnO_3$ shows the largest CMR effect among the manganites. Unlike what is expected from the FM phase Raman spectra of $Nd_{0.7}Sr_{0.3}MnO_3$ show the formation of fine structures in phonon modes upon cooling through T_C. The related local lattice distortions imply a strong carrier localization even in the low temperature metallic phase. The electronic response becomes stronger with decreasing temperature. This is ascribed to an enhancement of carrier scattering due to carrier delocalizations. The observation of the opposing tendency indicates the competition between the localization and the delocalization of carriers. Therefore, our results suggest that inhomogeneous magnetism and phase separation are significant at very low temperature of the FM phase. In the half-doped $Nd_{0.5}Sr_{0.5}MnO_3$ new phonon modes are observed below the charge-ordering temperature $T_{CO} = 148$ K. Their appearance is related to the presence of layered charge/orbital ordering. Moreover, upon cooling, these modes undergo a substantial hardening. The observed hardening points to the coexistence of an FM phase in the CE-type charge-/orbital-ordered state.

2. Experimental details

Single crystals of $Nd_{1-x}Sr_xMnO_3$ ($x = 0.3, 0.5$) used in this work were grown in an infrared image furnace by the floating zone technique. Further details about the crystal growth technique can be found elsewhere [14]. The samples were characterized by x-ray diffraction, resistivity and magnetization measurements. The Raman scattering measurements were carried out in a quasi-backscattering geometry with 5 mW of the excitation line $\lambda = 514.5$ nm of an Ar^+ laser. The spectra were analysed using a DILOR-XY spectrometer and a back-illuminated CCD detector.

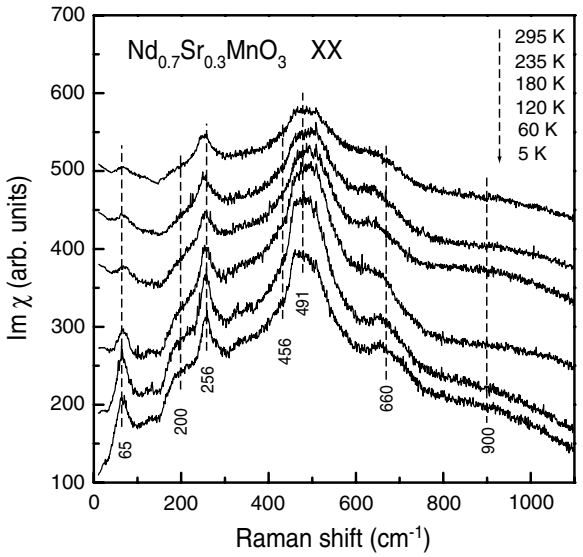

Figure 1. Raman spectra of $Nd_{0.7}Sr_{0.3}MnO_3$ in XX polarization at different temperatures. The raw data were corrected by the Bose–Einstein factor and shifted systematically for clarity. The broken vertical lines are guides for eyes.

3. Results and discussions

3.1. Raman spectra of $Nd_{0.7}Sr_{0.3}MnO_3$

The temperature dependence of Raman spectra at XX polarization is shown in figure 1. At 5 K we have observed phonon bands at 65 cm^{-1} (M_1), 200 cm^{-1} (M_2), 256 cm^{-1} (M_3), 456 cm^{-1} (M_4), 491 cm^{-1} (M_5) and 660 cm^{-1} (M_6). Note here that the raw Raman data are corrected by the Bose–Einstein thermal factor $\mathrm{Im}\,\chi = S(\omega)/[1 + n(\omega)]$, where $[1 + n(\omega)] = [1 - \exp(-\hbar\omega/k_BT)]^{-1}$. The six modes are phononic Raman scattering and part of 24 symmetry-allowed modes in the orthorhombic symmetry of the perovskite structure. These phonon peaks are superimposed on a broad electronic background. The modes are assigned by consulting earlier work [15] in which systematic Raman measurements and lattice dynamical calculations for orthorhombic $LaMnO_3$ are reported. The M_1 mode with A_g symmetry was believed to be a rotational mode. A recent oxygen isotope study [16], however, suggests that it is related to the vibration of Nd cations. The M_2 mode is ascribed to an in-phase rotational vibration of the MnO_6 octahedra about the y axis with A_g character. The M_3 mode corresponds to an out-of-phase rotation of the MnO_6 octahedra around the x axis. The M_4 band is associated with an out-of-phase bending mode of the oxygen cage with B_g character. The M_5 mode corresponds to an out-of-phase stretching vibrations of the octahedra and is associated with the JT distortion of the octahedra. The M_6 mode, called the breathing mode, is due to bending vibrations of octahedra. Usually, a divalent doping leads to a strong reduction of Raman scattering intensity of the last two modes because of a vanishing static JT distortion and screening effect by free carriers. In the studied system, though the breathing mode is very weak, the JT mode at 491 cm^{-1} is quite intense. This indicates the presence of a substantial JT distortion even in the low-temperature FM phase. The origin of the weak mode around 900 cm^{-1} will be discussed below.

We will now discuss the temperature dependence of the phonon modes. With lowering temperature through the MIT all phonon modes become more intense while additional

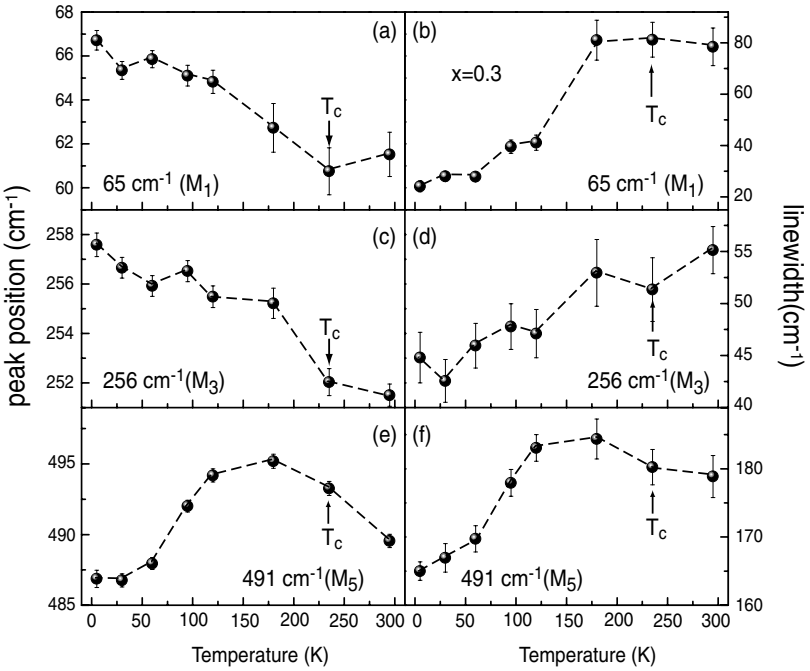

Figure 2. Temperature dependence of the peak position of the Raman frequency (a), (c), (e) and the full width at half maximum (b), (d), (f) for the 65, 256 and 491 cm^{-1} modes of $Nd_{0.7}Sr_{0.3}MnO_3$. The broken curves are guides for the eyes.

fine structures develop. At the same time, a broad electronic background becomes more pronounced. In the FM state the increased mobility of the charge carriers prevents forming a quasistatic lattice distortion around the Mn^{3+} sites while enhancing the electronic response. Furthermore, the screening effect of the delocalized carriers will strongly suppress all phonon modes. Actually, the increasing electronic continuum confirms the enhanced delocalization of carriers. But the observed phonon modes behave unlike what is expected in the FM phase. A continuous strengthening and narrowing of phonon modes up to 5 K is a typical behaviour of the ferromagnetic insulating phase accompanied by a formation of nuclei of a charge- (*or orbital*-) ordered state. In recent ^{55}Mn NMR measurements[18] a signal from an averaged Mn^{3+}/Mn^{4+} sites has been observed as well as independent Mn^{3+} and Mn^{4+} sites below T_C, pointing to strong carrier localization in the FM state. Furthermore, x-ray scattering measurements [10] show the presence of the CE-type COO state in the background of the FM state. However, such a localization has been observed only up to 0.7 T_c. In contrast, our results suggest that the FM phase is nonuniform even at lower temperature. Therefore, we conclude that phase segregation is significant not only just below T_C but also even in the very low temperature region where the DE mechanism is predominant.

To investigate quantitatively the evolution of peak frequencies and linewidths the spectra were fitted to a sum of Lorentzians after correcting for the Bose–Einstein thermal factor. The results are displayed in figure 2. Because of weak intensity the M_2, M_4 and M_6 modes will not be considered further. We noticed that there exists no hint for an asymmetric Fano lineshape which is expected from an interaction between the phonon mode and the electronic continuum. This implies that the density of free carriers is not high possibly due to strong carrier localization below T_C.

The temperature dependence of the peak frequency and linewidths for the M_1 and M_3 modes is shown in figures 2(a)–(d). Both modes exhibit a substantial hardening as the temperature is lowered from T_C to 5 K. Furthermore, a discontinuous change is observed around T_C. This hardening is larger than the usual phonon effects due to an anharmonicity of the lattice potential. Rather, this is caused by a combined effect of the DE and the electron–phonon interaction. In this mechanism the electronic bandwidth changes lead to a hardening of the phonon frequency and a reduction of the phonon damping [19]. This behaviour is well illustrated by the behaviour of the corresponding M_3 mode in the La-based manganites [20]. In the studied system, however, the abrupt change of the linewidth occurs in the temperature regime 120 K $< T <$ 180 K, that is, well below T_C. This indicates that the phonon modes are also damped by a coupling to spin degrees of freedom as indicated by an ordering of the MnO_6 octahedra below T_C [21]. The temperature dependence of the M_5 mode (the JT mode) shown in figures 2(e) and (f) is anomalous. As temperature is lowered, it hardens up to 150 K and then softens when approaching 5 K. The temperature dependence of the linewidth shows a similar behaviour. We will now consider a possible mechanism leading to the softening.

First, the softening and narrowing of the JT mode can result from a drastic change of JT lattice distortions through the MIT. Carrier delocalizations in the FM phase will reduce substantial distortions of the MnO_6 octahedra which are present in the PI phase. This leads to a weakening of the JT distortions and their corresponding vibrational energy in the FM phase. Noticeably, the softening begins to start around 180 K ($=0.75T_c$) at which the COO nanoclusters become disrupt [10]. This suggests that the softening is related to the disappearance of the short-range ordering of lattice distortions. Second, the softening can originate from a renormalization of phonon self-energy by magnetic moments, as reported in an anomalous softening of Mn–O bonding mode of $La_{0.725}Ca_{0.275}MnO_3$ [22]. In $Nd_{0.7}Sr_{0.3}MnO_3$ the local lattice distortions are correlated entities which are strongly coupled to the spin degrees of freedom [18]. Thus, the softening due to spin–phonon coupling should also be regarded as being relevant. Therefore, both mechanisms are taken into account simultaneously. Finally, we will mention recent theoretical studies [23, 24] which have proposed a phonon softening by orbital degrees of freedom: a softening can be triggered by the orbital fluctuating state and be controlled by the strength of the electron–phonon interactions. In this model, a softening implies the enhancement of electron–phonon coupling accompanying orbital order with increasing coherence length upon cooling. However, no evidence for the development of orbital ordering upon cooling has been reported until now. Thus, we rule out this possibility.

Now we will concentrate on the temperature dependence of the electronic background response observed in both the XX and the XY polarizations. A transition from the PI to the FM phase leads to a change of a broad electronic scattering from a diffusive response to a flat continuum response. The observed electronic Raman scattering can be understood within a collision-limited model [25]. When the carrier scattering rate is larger than the product of the wavevector and Fermi velocity ($\Gamma > qv_F$), for example due to strong electronic scattering from spins, impurities, phonons, etc, then one expects an appreciable electronic Raman response at low frequencies which is given by

$$\frac{\mathrm{d}^2\sigma}{\mathrm{d}\omega\,\mathrm{d}\Omega} \propto [1 + n(\omega)]\frac{B\omega\Gamma_L}{\omega^2 + \Gamma_L^2}$$

where $1 + n(\omega)$ is the Bose–Einstein thermal factor, B is the symmetry-dependent amplitude and Γ_L is the carrier scattering rate. In other manganites such a low frequency Raman response due to spin fluctuations and local lattice distortions, has been reported [21].

In the PI phase of the $Nd_{0.7}Sr_{0.3}MnO_3$ such a collision-dominated scattering is characterized by a diffusive behaviour seen as an elastic electronic Raman response below

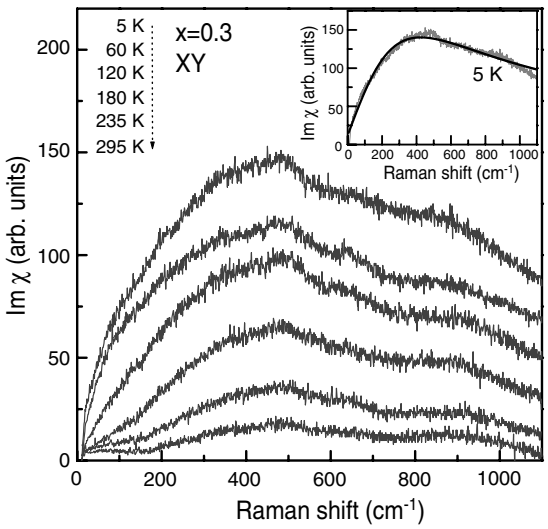

Figure 3. Raman spectra of $Nd_{0.7}Sr_{0.3}MnO_3$ in XY polarization at different temperatures. Inset: typical fit to a collision-dominated model at 5 K.

150 cm^{-1} as observed in the XX polarization (see figure 1). Noticeably, this low-frequency scattering is seen even at 180 K which lies well below T_c. This points to the presence of scattering from spin fluctuations or local lattice distortions in a substantial temperature range around T_c. Below T_c, in the metallic state, when electron–electron correlations increase, the scattering rate becomes frequency-dependent, $\Gamma(\omega, T) = \Gamma_0(T) + \alpha\omega^2$, within a Fermi liquid theory [26]. Here the parameter α denotes the electron correlation effects. This is related to a strongly correlated metallic phase dominated by strong inelastic carrier scattering from some broad spectrum of excitations. To analyse it quantitatively the XY spectrum which has negligible phonon contributions was fitted with the collision-dominated model. A typical fit is shown in the inset of figure 3 and the fitting results are summarized in figure 4.

Upon decreasing temperature up to 60 K the scattering rate of Γ_0 decreases nonlinearly and then slightly increases upon further cooling. The increase of Γ_0 below 60 K may originate from an enhancement of spin fluctuations due to the ordering of Nd spins below 20 K and a subsequent canting of Mn spins [27]. The observed $\Gamma_0 \approx 200$–400 cm^{-1} is much smaller than that of the large bandwidth manganite $La_{0.7}Sr_{0.3}MnO_3$ with $\Gamma_0 = 2100$ cm^{-1} [28]. This is because the DE mechanism of the latter is more effective due to the large ionic radius of the La atom. As a result, the carrier can hop more easily. An intermediate bandwidth manganite $Pr_{0.63}Sr_{0.37}MnO_3$ exhibits the smaller scattering rate of $\Gamma_0 = 40$ cm^{-1} despite a comparable bandwidth to the $Nd_{0.7}Sr_{0.3}MnO_3$ [29]. This discrepancy is due to the presence of an additional scattering channel on carrier disorder in $Nd_{0.7}Sr_{0.3}MnO_3$, for example, due to spin–spin fluctuations and an inhomogeneous FM state. In addition, the electron correlation coefficient of $\alpha \approx 2 \times 10^{-3}$ at 5 K disappears when approaching T_c. This shows that the MIT is related to a change of electronic correlations. The increasing Coulomb correlations with decreasing temperature would push most of the low frequency scattering upwards to the plasma edge as observed for EuO and EuB_6 [30]. Noticeably the weak mode around 900 cm^{-1} grows into a prominent one at low temperatures in both the XX and XY scattering geometry. This indicates that the 900 cm^{-1} mode may be understood in terms of a plasmon-like excitation. Usually, a plasmon-like excitation is expected to occur at the plasma frequency

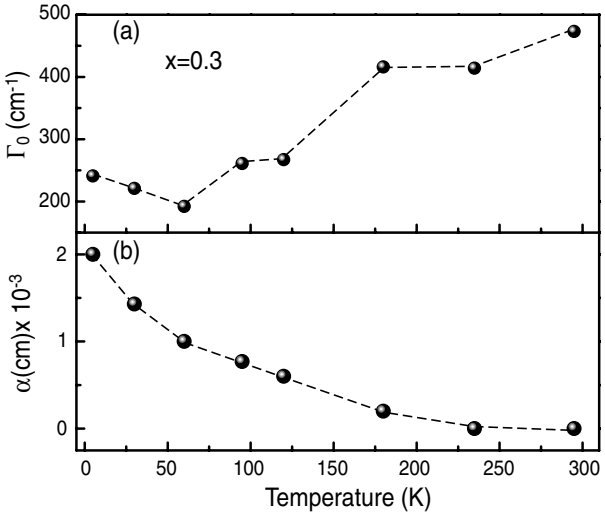

Figure 4. Temperature dependence of the fitted parameters obtained within the collision-dominated model for the XY Raman spectrum $Nd_{0.7}Sr_{0.3}MnO_3$: (a) frequency-independent scattering rate and (b) electron correlation constant. The broken curves are guides for the eyes.

$\omega_p = (ne^2/\epsilon_0 m^*)^{1/2}$ with electric charge e, carrier density n and effective mass m^*. The plasma edge of $\hbar\omega_p \sim 0.6$ eV obtained by optical conductivity measurements [31] is much higher than the observed energy of the M_7 mode. A large discrepancy between the Raman and infrared energy scales seems to indicate a two-component plasma with different carrier densities as proposed in [17]. In this case Raman spectroscopy is more sensitive to the low-frequency component as screening effects are less significant in this regime. Even though such a scenario is plausible, further studies are needed to substantiate its exact origin. The 900 cm^{-1} mode lies in the two-phonon energy region of the JT mode. Thus, as another explanation, higher-phonon scattering can be suggested.

3.2. Raman spectra of $Nd_{0.5}Sr_{0.5}MnO_3$

The temperature dependence of the Raman spectra of $Nd_{0.5}Sr_{0.5}MnO_3$ measured in the XX polarization is shown in figure 5. At room temperature the M_1, M_2 and M_4 modes have been observed. The two bands of the M_5 and M_6 modes are very weak because of negligible JT distortions caused by a larger concentration of Mn^{4+} ions. Upon cooling through the charge-ordering temperature $T_{CO} = 148$ K, the new modes M_{CO1} at 490 cm^{-1}, M_{CO2} at 612 cm^{-1} and M_{CO3} at 664 cm^{-1} develop. In addition, a weak fine structure around 334 and 402 cm^{-1} appears at lower temperature. Their intensity smoothly increases with increasing temperature. The appearance of new phonon modes can be ascribed to the ordering of Mn^{3+} and Mn^{4+} ions, leading to the freezing of the dynamical JT distortions into a superstructure with doubled lattice parameters. At high temperatures $Nd_{0.5}Sr_{0.5}MnO_3$ is a paramagnetic insulator ($Imma$). Upon cooling it undergoes a transition to a FM at $T_C = 250$ K without changing the crystal structure, and then to a CE-type charge-ordered insulator with the $d_{3x^2-r^2/3y^2-r^2}$ type orbital ordering ($P2_1/m$) [32]. For the $P2_1/m$ space group 54 Raman-active modes of $31A_g + 23\ B_g$ are expected. Thus, it is practically impossible to assign the observed modes to specific octahedral vibrations. Noticeably, however, the intense phonons which appear below T_{CO} have been observed in the Mn–O bending and stretching modes. Thus, instead of the actual $P2_1/m$

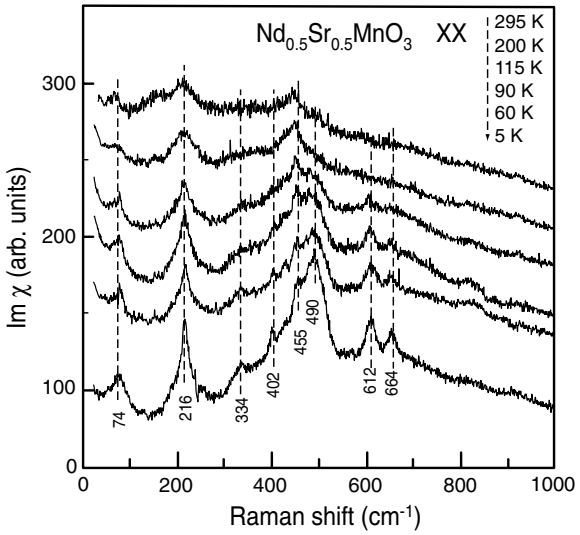

Figure 5. Temperature dependence of the Raman spectra of $Nd_{0.5}Sr_{0.5}MnO_3$ in the XX polarization. Note that the raw data are corrected by the Bose–Einstein factor and shifted for a better presentation. The broken vertical lines are guides for the eyes.

structure, we can consider a simplified *Pmma* structure ($a \approx 2\sqrt{2}a_p, b \approx a_p, c \approx \sqrt{2}a_p$) with charge and orbital ordering but without the octahedron tilt. To neglect the octahedra tilt is justified because the low-energy modes corresponding to the rotation of the octahedra undergo no substantial change through T_{CO}. Moreover, the intensive phonon bands seen below T_{CO} have corresponding lines in the COO layered manganites $La_{0.5}Sr_{1.5}MnO_4$ and $LaSr_2Mn_2O_7$ as well as in the half Ca-doped manganites $La_{0.5}Ca_{0.5}MnO_3$ which has the same CE-structure as $Nd_{0.5}Sr_{0.5}MnO_3$ [33, 34]. This enables us to conclude that the intensive phonon bands arise from charge and orbital ordering in the Mn–O layers.

The higher site symmetry of *Pmma* reduces the number of Raman-active modes to 18 consisting of $7A_g + 2B_{1g} + 7B_{2g} + 2B_{1g}$. The new intensive modes appearing below T_{CO} are related to vibration patterns of pairs of octahedra consisting of undistorted $Mn^{4+}O_6$ and JT distorted $Mn^{3+}O_6$ octahedra due to the checkboard-type charge order. We refer to [34] for a detailed assignment. Here we will briefly mention that the M_{CO1} and M_{CO2} modes originate from the charge ordering alone while the M_{CO3} mode is due to the concomitant charge and orbital ordering. This can be understood as follows. If we assume that only charge ordering takes place without orbital ordering, then the crystal symmetry of *Pmma* becomes *Pnma* ($a \approx \sqrt{2}a_p, b \approx a_p, c \approx \sqrt{2}a_p$) which has the same space group as $LaMnO_3$/$YMnO_3$. The M_{CO1} mode has a corresponding line in $YMnO_3$ while M_{CO2} has a corresponding line in $LaMnO_3$ [15, 34]. In contrast, the M_{CO3} has no corresponding line in $LaMnO_3$/$YMnO_3$. Thus, its presence should be caused by orbital/charge ordering.

Finally, we will consider the temperature dependence of the peak position of the M_{CO1}, M_{CO2} and M_{CO3} modes. M_{CO1} is observed as a weak shoulder of the M_4 mode, even above T_{CO}. This points to the existence of charge/orbital correlations above T_{CO}. This is consistent with the observation of short-range orbital ordering in the FM phase by hard x-ray scattering measurements [13]. As displayed in figure 6, upon cooling below 115 K all three modes harden strongly and then saturate at low temperatures. The hardening amounts to 2–11 cm^{-1}. Below T_{CO} the A-type AF and FM phases with their associated crystal structures coexist with

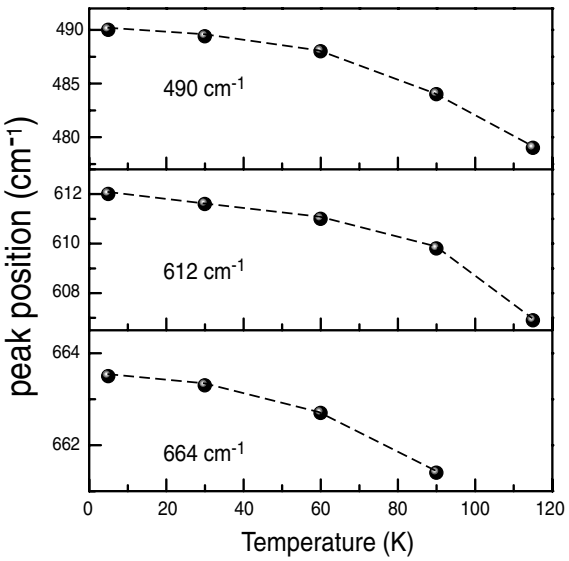

Figure 6. Temperature dependence of the peak position of three phonon modes which appear below the charge-ordering temperature $T_{CO} = 148$ K. The analysis of the M_{CO1} mode is restricted to temperatures below 115 K due to its weak intensity. The broken curves are guides for the eyes.

the CE-phase [12]. This motivates us to interpret the hardening in terms of frequency shifts due to spin–phonon effects. Usually, the shift of phonon frequency is proportional to the square of the ordered magnetic moment [35]. If the ordered moment increases upon cooling the phonons soften. In contrast, when the magnetic moment decreases upon cooling the phonons harden. Thus, the hardening can be translated into a reduction of magnetic moment with decreasing temperature. In other words, a fraction of the FM phase in the CE-phase decreases gradually with lowering temperature through T_{CO} and then disappears at low temperatures. ^{55}Mn spin-echo ferromagnetic nuclear resonance has been observed down to 70 K [18]. Therefore, we can conclude that the coexistence of the FM and AFM phases persists down to around 70 K.

4. Conclusions

We have presented an inelastic light scattering study of single-crystals $Nd_{1-x}Sr_xMnO_3$ with $x = 0.3$ and 0.5. Raman spectra of $Nd_{0.7}Sr_{0.3}MnO_3$ undergo a substantial change through the MIT: with decreasing temperature all phonon modes grow in intensity and additional weak modes appear. This points to the persistence of local JT lattice distortions and the presence of nuclei of the charge-ordered state at very low temperatures which tend to localize carriers. This result signals the importance of inhomogeneity even at lower temperatures than where ^{55}Mn NMR measurements and x-ray scatterings have reported [10, 18]. In contrast, the electronic continuum exhibits a continuous increase pointing to carrier delocalizations. Therefore, our results indicate a phase segregation which is consistent with a strong competition between carrier localization and carrier delocalization in the FM phase of $Nd_{0.7}Sr_{0.3}MnO_3$. Raman spectra of the half-doped $Nd_{0.5}Sr_{0.5}MnO_3$ also exhibit a significant change through the charge ordering. Below T_{CO} the most intensive three lines appear due to charge/orbital ordering of Mn–O layers. Substantial hardening which results from the coexistence of the FM and CE-phases is interpreted as a gradual reduction of a fraction of the FM phase in the CE-phase upon cooling below T_{CO}.

Acknowledgments

The work was supported by a grant from the EPSRC, UK in the UK and by DFG/SPP 1073 in Germany and NATO Collaborative Linkage Grant PST. CLG. 977766.

References

[1] Tokura Y (ed) 2000 *Colossal Magnetoresistive Oxides* (London: Gordon and Breach)
[2] Millis A J 1998 *Nature* **392** 147
[3] Zener C 1951 *Phys. Rev.* **82** 403
[4] Millis A J, Littlewood P B and Shraiman B I 1995 *Phys. Rev. Lett.* **74** 5144
[5] Goodenough J B 1955 *Phys. Rev.* **100** 564
Goodenough J B, Wold A, Arnott R J and Menyuk N 1961 *Phys. Rev.* **124** 373
[6] van den Brink J, Khaliullin G and Khomskii D 2002 *Preprint* cond-mat/0206053
[7] Dagotto E, Hotta T and Moreo A 2001 *Phys. Rep.* **344** 1
[8] Xiong C, Li Q, Ju H L, Mao S L, Senapati L, Xi X X, Greene R L and Venkatesan T 1995 *Appl. Phys. Lett.* **66** 1427
[9] Caignaert, Maignan A and Raveau B 1995 *Solid State Commun.* **95** 357
[10] Koo T Y, Kiryukhin V, Sharma P A, Hill J P and Cheong S-W 2001 *Phys. Rev.* B **64** 220405
[11] Fujiwara T and Korotin M 1999 *Phys. Rev.* B **59** 9903
[12] Kiryukhin V, Kim B G, Katsufuji T, Hill J P and Cheong S-W 2001 *Phys. Rev.* B **63** 144406
[13] Geck J, Bruns D, Hess C, Klingeler R, Reutler P, v Zimmenermann M, Cheong S-W and Büchner B 2002 *Phys. Rev.* B **66** 184407
[14] Paul D McK, Kamenev K V, Campbell A J, Balakrishnan G, Less M R and McIntyre G J 1998 *Phil. Trans. R. Soc.* **356** 1543
[15] Iliev M N, Abrashev M V, Lee H-G, Povov V N, Sun Y Y, Thomsen C, Meng R L and Chu C W 1998 *Phys. Rev.* B **57** 2872
[16] Amelitchev V A, Guettler B, Gorbenko O Yu, Kaul A R, Bosak A A and Ganin A Yu 2001 *Phys. Rev.* B **63** 104430
[17] Bjoernsson P, Ruebhausen M, Baeckstroem J, Kaell M, Eriksson S, Eriksen J and Boerjesson L 2000 *Phys. Rev.* B **61** 1193
[18] Pattabiraman M, Murugaraj P, Rangarajan G, Dimitropoulos C, Ansermet J-Ph, Papavassiliou G, Balakrishnan G, Paul D McK and Lees M R 2002 *Phys. Rev.* B **66** 224415
[19] Lee J D and Min B I 1997 *Phys. Rev.* B **55** 12454
[20] Irwin J C, Chrzanowski J and Franck J P 1999 *Phys. Rev.* B **59** 9362
[21] Yoon S, Liu H L, Schollerer G, Cooper S L, Han P D, Payne D A, Cheong S-W and Fisk Z 1998 *Phys. Rev.* B **58** 2795
[22] Pantoja A E, Trodahl H J, Buckley R G, Tomioka Y and Tokura Y 2001 *J. Phys.: Condens. Matter* **13** 3741
[23] van den Brink J 2001 *Phys. Rev. Lett.* **87** 217202
[24] Bala J, Oleś A and Sawatzky G 2002 *Phys. Rev.* B **65** 184414
[25] Zawadowski A and Cardona M 1990 *Phys. Rev.* B **42** 10732
[26] Pines D 1963 *Elementary Excitations in Solids* (New York: Addison-Wesley)
[27] Park J, Kim M S, Park J-G, Swainson I P, Ri H-C, Lee H J, Kim K H, Noh T W, Cheong S-W and Lee C 2000 *J. Korean Phys. Soc.* **36** 412
[28] Gupta R, Sood A K, Mahesh R and Rao C N R 1996 *Phys. Rev.* B **54** 14899
[29] Liu H L, Yoon S, Cooper S L, Cheong S-W, Han P D and Payne D A 1998 *Phys. Rev.* B **58** R10115
[30] Snow C S, Cooper S L, Young D P, Fisk Z, Comment A and Ansermet J-Ph 2001 *Phys. Rev.* B **64** 174412
[31] Lee H J, Jung J H, Lee Y S, Ahn J S, Noh T W, Kim K H and Cheong S-W 1999 *Phys. Rev.* B **60** 5251
[32] Ritter C, Mahendiran R, Ibarra M R, Morellon L, Maignan A, Raveau B and Rao C N R 2000 *Phys. Rev.* B **61** R9229
[33] Yamamoto K, Kimura T, Ishikawa T, Katsufuji T and Tokura Y 2000 *Phys. Rev.* B **61** 14706
[34] Abrashev M V, Bäckström J, Börjesson L, Pissas M, Kolev N and Iliev M N 2001 *Phys. Rev.* B **64** 144429
[35] Baltensperger W and Helman J S 1968 *Helv. Phys. Acta* **41** 668